J|A|C|S ARTICLES

Published on Web 04/14/2009

Differentiating Solvation Mechanisms at Polar Solid/Liquid Interfaces

Michael R. Brindza[†] and Robert A. Walker[†,‡,*]

Department of Chemistry and Biochemistry, University of Maryland, College Park, Maryland 20742

Received December 29, 2008; E-mail: rawalker@umd.edu

Abstract: Resonance enhanced second harmonic generation (SHG) has been used to identify solvation mechanisms at different solid/liquid interfaces. Solvation interactions are characterized as being either nonspecific and averaged over the entire solute cavity or specific, referring to localized, directional interactions between a solute and its surroundings. SHG spectra report the electronic structure of solutes adsorbed to silica/organic solvent interfaces, and different solutes are chosen to probe either interfacial polarity or interfacial hydrogen bond donating/accepting opportunities. SHG results show that interfacial polarity probed by *p*-nitroanisole depends sensitively on solvent structure, whereas hydrogen bonding interactions probed by indoline are insensitive to solvent identity and instead are dominated by the hydrogen bond donating properties of the polar silica substrate. The bulk solvation interactions were modeled with a series of *ab initio* calculations that characterized solute electronic structure within a dielectric continuum and in the presence of explicit, individual solvent molecules. Collectively, these measurements and calculations create a comprehensive picture of how solvation mechanisms vary at different polar, solid surfaces.

1. Introduction

Solvation at solid/liquid interfaces will differ from bulk solution limits due to a solute's interactions with the substrate as well as the structural and dynamic changes induced by the substrate in the adjacent solvent. Given that surface mediated solvation will control solute concentration, structure, and reactivity at interfaces, understanding the effects of a surface on solvation is essential for predicting solution-phase surface chemistry. Numerous studies have shown that different solute properties near solid/liquid interfaces can depend on solvent structure, surface composition, and solute identity.[1−12] However, many of these reports vary only a limited number of parameters, and the resulting interpretation provides only a partial picture of how the chemical asymmetry found at surfaces leads to unique interfacial environments. Experiments described below examine how solvation mechanisms vary at interfaces formed between organic liquids and polar silica surfaces. Specifically, solutes are chosen to probe independently interfacial polarity and hydrogen bonding. Results show that solvent polarity depends sensitively on solvent structure, whereas hydrogen bonding opportunities remain largely independent of solvent identity, even when the solvent itself can form strong hydrogen bonds.

In this work, we characterize solvation as being either nonspecific or specific.[13−15] Nonspecific solvation refers to solvent−solute interactions that are averaged over the entire solute cavity. Solvent polarity stands out as an example of this type of solvation. When considering polarity, one treats the solvent as an effective polarizable continuum around an overall solute dipole. Polarity itself lacks a rigorous, quantitative definition and includes a sum over all noncovalent interactions experienced between a solute and its surroundings. Nevertheless, numerous theoretical and empirical scales have emerged to characterize this property, and in recent years simulations have attempted to isolate contributions made by solvent dipolar and dispersion forces to a solute's electronic structure.[16−19] In contrast to solvent polarity, specific solvation describes solvent−solute interactions that are localized and directional. Examples of this type of solvation include dipole−dipole,

[†] Department of Chemistry and Biochemistry, University of Maryland.
[‡] Chemical Physics Program, University of Maryland.

(1) Lynden-Bell, R. M.; Del Popolo, M. G.; Youngs, T. G. A.; Kohanoff, J.; Hanke, C. G.; Harper, J. B.; Pinilla, C. C. *Acc. Chem. Res.* **2007**, *40*, 1138.
(2) Tavana, H.; Neumann, A. W. *Adv. Colloid Interface Sci.* **2007**, *132*, 1.
(3) Li, I.; Bandara, J.; Shultz, M. J. *Langmuir* **2004**, *20*, 10474.
(4) Farrer, R. A.; Fourkas, J. T. *Acc. Chem. Res.* **2003**, *36*, 605.
(5) Lee, S. H.; Rossky, P. J. *J. Chem. Phys.* **1994**, *100*, 3334.
(6) Ribarsky, M. W.; Landman, U. *J. Chem. Phys.* **1992**, *97*, 1937.
(7) Al-Abadleh, H. A.; Mifflin, A. L.; Bertin, P. A.; Nguyen, S. T.; Geiger, F. M. *J. Phys. Chem. B* **2005**, *109*, 9691.
(8) Doerr, A. K.; Tolan, M.; Schlomka, J. P.; Press, W. *Europhys. Lett.* **2000**, *52*, 330.
(9) Eisenthal, K. B. *Chem. Rev.* **1996**, *96*, 1343.
(10) Shang, X. M.; Benderskii, A. V.; Eisenthal, K. B. *J. Phys. Chem. B* **2001**, *105*, 11578.
(11) Zhang, X. Y.; Cunningham, M. M.; Walker, R. A. *J. Phys. Chem. B* **2003**, *107*, 3183.
(12) Zhang, X. Y.; Walker, R. A. *Langmuir* **2001**, *17*, 4486.
(13) Catalan, J. *J. Org. Chem.* **1997**, *62*, 8231.
(14) *Quantitative treatments of solute/solvent interactions*; Politzer, P., Murray, J. S. Eds.; Elsevier: Amsterdam, 1994; p 368.
(15) Suppan, P. *J. Photochem. Photobiol., A* **1990**, *50*, 293.
(16) Buncel, E.; Rajagopal, S. *Acc. Chem. Res.* **1990**, *23*, 226.
(17) Catalan, J. *J. Org. Chem.* **1995**, *60*, 8315.
(18) Laurence, C.; Nicolet, P.; Dalati, M. T.; Abboud, J. L. M.; Notario, R. *J. Phys. Chem.* **1994**, *98*, 5807.
(19) Matyushov, D. V.; Schmid, R.; Ladanyi, B. M. *J. Phys. Chem. B* **1997**, *101*, 1035.

charge−dipole, and hydrogen bonding interactions. Again, many studies have proposed empirical scales to treat the effects of specific solvation interactions on solute chemistry, but only a few of these efforts have resulted in models that are sufficiently general to cover a variety of solutes solvated by many different classes of solvents.[13,20−22]

At solid/liquid interfaces one expects both nonspecific and specific solvation interactions to be different than in bulk solution. First, depending on the magnitudes and types of interactions, interfacial solute concentrations may be enhanced through adsorption or depleted by unfavorable energetics (such as Coulomb repulsions or hydrophobic effects).[23−26] Second, the surface itself will alter a solvent's density, local dielectric constant, and viscosity, thereby changing solvent−solute interactions across the anisotropic, interfacial region.[6,8,27−31] These effects—direct substrate/solute interactions and substrate induced changes in solvent properties—can have consequences for a multitude of technologically and biophysically relevant phenomena. For example, attractive substrate−solute interactions can be tailored to drive the assembly of well-ordered arrays of adsorbates at the solid/liquid interface. Such systems can include functionalized electrodes and thin films constructed specifically to serve as sensors.[32,33] Creation of an organized assembly requires that the overall change in system free energy be favorable but often necessitates overcoming specific individual interactions (such as arrays of parallel aligned dipoles or like-charges) that are energetically (or entropically) destabilizing. If, however, the surface also enhances interfacial solvation interactions, effectively screening adsorbed solutes from each other, then such self-assembled species can enjoy greater structural and organizational uniformity.

A second example of how different types of solvation can impact interfacial processes comes from the general area of chromatography. Adsorption to silica surfaces has been investigated intensively for decades.[34−37] These studies have led to a detailed understanding of how chemisorbed solutes aggregate on silica surfaces as well as empirical procedures designed to functionalize these surfaces and minimize the chromatographic tailing. In reversed phase chromatography columns, the silica is treated with an alkylating agent to reduce the number of surface silanol groups.[37] Large scale industrial applications motivate manufacturers to go to great lengths to "cap" these hydrogen bonding sites with small alkyl silanes. Still, researchers propose that uncapped, acidic silanol groups and topographical inhomogeneities bear responsibility for retaining more basic analytes through hydrogen bond donation *from* the silanol to the adsorbed solute.[36,38−41]

In the experiments described below, resonance enhanced second harmonic generation (SHG) is employed to examine specific and nonspecific solvation properties at solid/liquid interfaces formed between hydrophilic silica and different organic liquids. Complementing these measurements are a series of *ab initio* calculations intended to isolate and quantify the role played by different intermolecular interactions contributing to solvation. Experiments measure the solvatochromic behavior of both pNAs and indoline adsorbed to these boundaries, and results show that polarity varies considerably with solvent structure, but hydrogen bonding appears to be controlled primarily by solute/substrate interactions. In particular, interfaces formed between silica and alkanes are more polar than bulk solution, but the quantitative change(s) in the local dielectric environment correlate with solvent packing efficiencies (as inferred from bulk densities, melting points, and previously reported X-ray scattering studies).[8,30] Strongly associating solvents such as alcohols create a heterogeneous distribution of polarities across the interface implying the existence of anisotropic, ordered Langmuir film-like structures.[11,12] In contrast to the solvent-dependent polarity results, specific solvation experienced by indoline at these same interfaces is dominated by the hydrogen bond donating properties of the solid surface, regardless of solvent identity. Only by rendering the silica surface hydrophobic are specific solvation forces changed at the solid/liquid interface.

2. Experimental Section

To establish benchmark solvent−solute interactions in bulk solution, absorbance spectra of the solutes in different solvents were acquired using a Hitachi U-3010 spectrophotometer, with 1 nm resolution. Solution concentrations were adjusted such that the maximum absorbances were between 0.1 and 1.0. Figure 1 shows the absorbance maxima corresponding to the lowest allowed electronic excitations of *p*-nitroanisole (pNAs) and indoline in a variety of solvents. The solvents are distinguished by their Onsager polarity functions $f(\epsilon)$[42]

$$f(\varepsilon) = \frac{2(\varepsilon - 1)}{(2\varepsilon + 1)} \tag{1}$$

where ϵ is a solvent's static dielectric constant. (Table 1) pNAs is sensitive to nonspecific solvation forces as evidenced by an excitation wavelength that increases monotonically from 293 to 317 nm as solvent polarity increases from that of alkanes ($\epsilon = 2.0$, $f(\epsilon) = 0.40$) to that of water and DMSO ($\epsilon_{H_2O} = 78$, $f(\epsilon)_{H2O} = 0.98$; $\epsilon_{DMSO} = 37$, $f(\epsilon)_{DMSO} = 0.96$) (Figure 2, top). In contrast, λ_{max} of indoline is insensitive to polarity, remaining near 300 nm for a collection of solvents varying in polarity from alkanes to acetonitrile (ACN). When indoline is dissolved in DMSO, however, λ_{max} shifts to 307 nm, and in H_2O (pH = 6.2), λ_{max} of indoline falls to 288 nm (Figure 1, bottom). While ACN, DMSO, and H_2O have similar polarities—$f(\epsilon) = 0.96-0.98$ for the three solvents—ACN is a poor

(20) Bayliss, N. S.; McRae, E. G. *J. Phys. Chem.* **1954**, *58*, 1002.
(21) Esenturk, O.; Walker, R. A. *Phys. Chem. Chem. Phys.* **2003**, *5*, 2020.
(22) Kamlet, M. J.; Abboud, J. L. M.; Abraham, M. H.; Taft, R. W. *J. Org. Chem.* **1983**, *48*, 2877.
(23) Somasundaran, P.; Shrotri, S.; Huang, L. *Pure Appl. Chem.* **1998**, *70*, 621.
(24) Shafir, A.; Andelman, D.; Netz, R. R. *J. Chem. Phys.* **2003**, *119*, 2355.
(25) Hayes, P. L.; Gibbs-Davis, J. M.; Musorrafiti, M. J.; Mifflin, A. L.; Scheidt, K. A.; Geiger, F. M. *J. Phys. Chem. C* **2007**, *111*, 8796.
(26) Hayes, P. L.; Malin, J. N.; Konek, C. T.; Geiger, F. M. *J. Phys. Chem. A* **2008**, *112*, 660.
(27) Lum, K.; Chandler, D.; Weeks, J. D. *J. Phys. Chem. B* **1999**, *103*, 4570.
(28) MacRitchie, F. *Chemistry at Interfaces*; Academic Press: New York, 1990.
(29) Manne, S.; Gaub, H. E. *Science* **1995**, *270*, 1480.
(30) Yu, C. J.; Evmenenko, G.; Richter, A. G.; Datta, A.; Kmetko, J.; Dutta, P. *Appl. Surf. Sci.* **2001**, *182*, 231.
(31) Zhang, X.; Steel, W. H.; Walker, R. A. *J. Phys. Chem. B* **2003**, *107*, 3829.
(32) *Israelachvili Intermolecular and Surface Forces*, 2nd ed.; Academic Press: New York, 1992.
(33) Rusling, J. F.; Nassar, A. E. F. *J. Am. Chem. Soc.* **1993**, *115*, 11891.
(34) Iler, R. K. *The Chemistry of Silica*; Wiley: New York, 1979.
(35) Wirth, M. J.; Legg, M. A. *Annu. Rev. Phys. Chem.* **2007**, *58*, 489.
(36) Wong, A. L.; Harris, J. M. *J. Phys. Chem.* **1991**, *95*, 5895.
(37) Gilroy, J. J.; Dolan, J. W.; Snyder, L. R. *J. Chromatogr., A* **2003**, *1000*, 757.
(38) Hansen, R. L.; Harris, J. M. *Anal. Chem.* **1995**, *67*, 492.
(39) Kovaleski, J. M.; Wirth, M. *J. Anal. Chem.* **1997**, *69*, A600.
(40) Kovaleski, J. M.; Wirth, M. J. *J. Phys. Chem. B* **1997**, *101*, 5545.
(41) Smith, E. A.; Wirth, M. J. *J. Chromatogr., A* **2004**, *1060*, 127.
(42) Onsager, L. *J. Am. Chem. Soc.* **1936**, *58*, 1486.

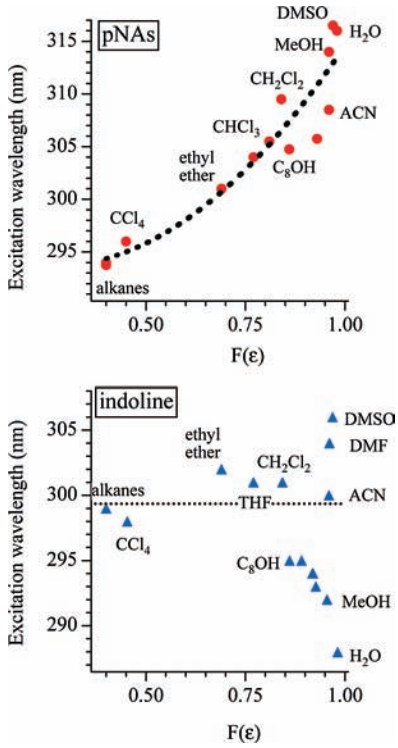

Figure 1. Solvatochromic activity of pNAs and indoline in various bulk solvents. Excitation wavelengths are plotted as a function of solvent's Onsager polarity function defined in eq 1. Uncertainties in excitation maxima are ±1 nm. Line widths in solution vary between 30 − 40 nm.

Table 1. Polarity Data and Excitation Wavelengths *p*-Nitroanisole (pNAs) and Indoline in Different Solvents[a]

			λ (bulk, nm)		λ (calculated, nm)	
solvent	ϵ	f(e)	pNAs	indoline	pNAs	indoline
cyclohexane	2.04	0.41	293	299	321.3	304.6
methyl-cyclohexane	2.03	0.41	294	299		
CCl_4	2.24	0.45	294	298		
ethyl ether	4.20	0.68	300	302		
chloroform	4.89	0.72	310	299		
methylene chloride	8.93	0.8	309	301		
1-octanol	10.3	0.86	304	295		
1-propanol	20.5	0.93	307	293		
methanol	32.7	0.95	313	292		295.6
acetonitrile	35.9	0.96	308	300		305.8
DMSO	46.5	0.97	317	307		313.4
water	78.4	0.98	317	288	336.9	294.7

[a] Solvatochromic data for pNAs and indoline in selected solvents. Onsager polarity functions ($f(\epsilon)$) were calculated according to ref 42. Calculated wavelengths were determined using a polarizable continuum model (IEFPCM) as described in the text. In the case of indoline, the DMSO and water calculations also included an explicit solvent molecule inside of the solute cavity as described in the text.

hydrogen bonding solvent, DMSO is a strong hydrogen-bond accepting solvent, and H_2O can both accept *and* donate hydrogen bonds. The hydrogen bond donating ability of H_2O is responsible for the dramatic shift to a shorter wavelength for λ_{max} as will be discussed in section 3.

To measure solvation interactions at solid/liquid interfaces, resonance enhanced SHG was used to acquire effective excitation spectra of adsorbed solutes. SHG is a second-order, nonlinear optical (NLO) technique that is inherently surface specific.[9,43,44] A number

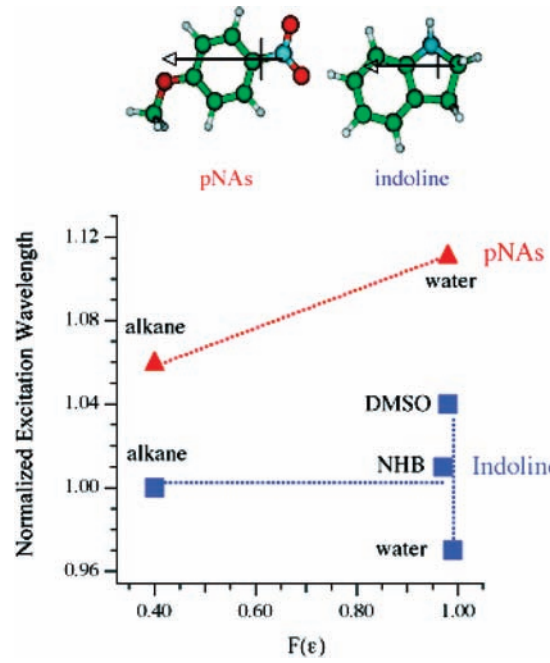

Figure 2. Normalized transition wavelengths for pNAs in different solvents as determined from *ab initio* calculations described in the text. NHB stands for a polarizable continuum without any explicit solvent molecules in the solute cavity capable of accepting or donating hydrogen bonds. Reported normalized wavelengths are scaled to the calculated gas phase transition wavelengths. (A normalized wavelength of 1.00 coincides with the gas phase limit.) Also shown are the molecular structures with the $S-S_1$ transition dipole vectors superimposed.

of studies have used SHG to report solvatochromic shifts of solutes adsorbed to liquid interfaces,[11,45−47] and Wang et al. used solvatochromic activity measured by SHG to develop a generalized interfacial polarity scale.[48] SHG relies on the generation of a second-order polarization by an incident oscillating electromagnetic field. The second harmonic field is proportional to the square of the incident field:

$$P^{(2)}(2\omega) = \chi^{(2)}E(\omega)^2 \tag{2}$$

where $\chi^{(2)}$ is the sample's macroscopic second-order susceptibility. This third ranked tensor contains all of the information related to the spatially averaged hyperpolarizability of molecules at surfaces and, under the electric dipole approximation, is zero in isotropic media. The tensor contains both resonant and nonresonant contributions:

$$\chi^{(2)} = \chi_R^{(2)} + \chi_{NR}^{(2)} \tag{3}$$

Typically, the resonant portion is much larger than the nonresonant term, and can be expressed as a function of real and virtual excitation energies:

$$\chi_R^{(2)} = \sum_{k,e} \frac{\mu_{gk}\mu_{ke}\mu_{eg}}{(\omega_{gk} - \omega - i\Gamma)(\omega_{eg} - 2\omega + i\Gamma)} \tag{4}$$

where μ_{ij} is the transition matrix element between two states i and j. The intensity of the second harmonic field depends quadratically

(43) Zhuang, X.; Miranda, P. B.; Kim, D.; Shen, Y. R. *Phys. Rev. B* **1999**, *59*, 12632.
(44) Wang, H. F.; Gan, W.; Lu, R.; Rao, Y.; Wu, B. H. *Int. Rev. Phys. Chem.* **2005**, *24*, 191.
(45) Steinhurst, D. A.; Owrutsky, J. C. *J. Phys. Chem. B* **2001**, *105*, 3062.
(46) TamburelloLuca, A. A.; Hebert, P.; Brevet, P. F.; Girault, H. H. *J. Chem. Soc., Faraday Trans.* **1996**, *92*, 3079.
(47) Wang, H. F.; Borguet, E.; Eisenthal, K. B. *J. Phys. Chem. A* **1997**, *101*, 713.
(48) Wang, H. F.; Borguet, E.; Eisenthal, K. B. *J. Phys. Chem. B* **1998**, *102*, 4927.

on the incident light intensity and the squared magnitude of the nonlinear susceptibility.

$$I_{2\omega} \propto |P^{(2)}|^2 = |\chi^{(2)}|^2 \cdot I_\omega^2 \quad (5)$$

By scanning the incident wavelength and monitoring the intensity of the coherently scattered second harmonic signal, experiments can measure effective excitation spectra of solute molecules in the anisotropic environment presented by liquid interfaces.

SHG experiments in these studies were conducted with a variety of solutions consisting of pNAs or indoline dissolved in organic solvents that were then brought into contact with a hydrophilic or hydrophobic silica prism. The solutes were purchased from Aldrich and used without further purification. (Reported purities were 99% for indoline, ≥ 97% for pNAs with major contaminants being structural isomers.) The SHG cell and detection assembly has been described previously.[11,12,31,49] For experiments requiring a hydrophilic silica surface the prism was cleaned in a 50/50 mixture (by volume) of sulfuric and nitric acids for several hours, thoroughly rinsed with deionized water (Millipore), and allowed to dry under N_2. Given that all experiments were carried out with solvents that contained varying amounts of dissolved H_2O, no additional efforts were made to remove any H_2O film that likely remained adsorbed to the hydrophilic silica surface. For experiments requiring a hydrophobic surface, the prism was cleaned in a similar fashion and then exposed to dichlorodimethylsilane vapor overnight. Static contact angle measurements with water showed angles in excess of 100° in agreement with literature reports.[50] (See Supporting Information for picture.) All SHG spectra were collected at a temperature of 21 ± 1 °C. Solution concentrations ranged from 50 to 100 mM for both solutes in alkanes, 200 mM in alcohols, and 200 mM for indoline in cyclohexane for measurement at the hydrophobic silica interface. These concentrations were necessary to acquire measurable SHG data. Smaller concentrations led to anticipated reductions in signal intensity but not to qualitative changes in electronic resonance wavelengths or band shapes.

The SHG apparatus uses the 1 kHz output of a Ti:sapphire regeneratively amplified, femtosecond laser (Clark-MXR CPA 2001, 130 fs pulse duration, 700 μJ). The output of the Ti:sapphire laser pumps a commercially available visible optical parametric amplifier (OPA, Clark-MXR). The visible output of the OPA is tunable from 550 to 700 nm with a bandwidth of 2.5 ± 0.5 nm. The polarization of the incident beam is controlled using a Glan-Taylor polarizer and a half wave plate. The fundamental 775 nm and any SH light generated from preceding optics are blocked with a series of filters prior to the detector. The incident light impinges on the interface at an angle of 68° relative to the surface normal, and the second harmonic response is detected in reflection using photon counting electronics. A second polarizer selects the SH polarization, and a short pass filter and monochromator serve to separate the signal from background radiation due to scattering or fluorescence.

All reported spectra were collected using p-polarized incident light and passing a p-polarized second harmonic signal. SH signals were normalized for incident power, and care was taken to confirm the quadratic behavior of $I(2\omega)$ on $I(\omega)$ at all wavelengths. Spectra shown in this work represent the average of 2−4 separate experiments acquired on separate days with new solutions and freshly cleaned cells. Each data point in a spectrum represents the average of at least three 10 s integrations of the detected SHG signal.

In addition to interfacial solvation, the average orientations of pNAs and indoline adsorbed to representative solid/liquid interfaces were determined from the polarization dependent second harmonic response. Following established protocols, the data enabled us to determine three unique, nonzero elements of $\chi^{(2)}$, χ_{XXZ}, χ_{ZXX}, and χ_{ZZZ}. These data were coupled with calculated hyperpolarizabilities to estimate averaged adsorbate orientations at both alkane/silica and alcohol/silica interfaces using well developed methods reported in the literature.[43,44,51] *Ab initio* methods (Gaussian 03[52]) were also used to calculate electronic transition energies of pNAs and indoline in a cavity surrounded by a polarizable continuum characterized by a static dielectric constant, ϵ. Where hydrogen bonding might be expected, explicit solvent molecules were included in the cavity itself to simulate specific solvent−solute interactions. To model the experimental results, we performed a series of calculations using time dependent density functional theory (TDDFT) to determine excitation energies in cavities created within a polarizable continuum model (IEFPCM). Solvent systems were chosen to model results from experiments, namely, pNAs in nonpolar and polar cavities, indoline in nonpolar and polar cavities, and indoline in polar cavities with explicit water and DMSO solvent molecules included to capture the effects of hydrogen bond donation and acceptance. pNAs and indoline's gas phase geometries were optimized for the lowest energy structure at the MP2 level of theory using a 6-31G(d) basis set. After geometry optimization a TDDFT calculation was performed with the BLYP functional and 6-31+G(d,p) basis set to determine the electronic transition wavelengths and hyperpolarizabilities. Due to a systematic error in excitation energies, we normalized the frequencies to the gas phase calculation limit to enable comparison with experimental results (Table 1). Determining the hyperpolarizabilities of pNAs and indoline required using an HF level of theory with a 6-31+G(d,p) basis set and the POLAR = EnOnly keyword. All calculations were performed using Gaussian 03.[52]

3. Results

3.1. Electronic Structure Calculations. Experimental and calculated solute transition wavelengths and solvatochromic activity are reported in Table 1. Since the electronic structure of pNAs is sensitive only to solvent polarity, calculations of this solute's electronic structure were carried out without explicit solvent molecules in the cavity. Given indoline's polarity-independent electronic structure, calculations for this solute required the presence of explicit solvent molecules to replicate solute electronic structure in hydrogen bond donating and hydrogen bond accepting environments. DMSO can only accept H-bonds. Water can both accept and donate hydrogen bonds, but reported calculations of the negative enthalpies of hydrogen bond formation show that the hydrogen bond donated by H_2O to related phenols is much stronger than the hydrogen bond formed with H_2O as the hydrogen bond acceptor.[53−55]

Figure 2 shows optimized, gas-phase structures of pNAs and indoline as well as the scaled, calculated wavelengths of both solutes in representative solvent environments. The calculated solvatochromic data are also summarized in Table 1. The computational results reported in Figure 2 and Table 1 reflect clearly the trends observed experimentally and reported in Figure 1, namely that pNAs exhibits a pronounced red shift in excitation wavelength with increasing polarity, whereas the indoline electronic structure depends little on its local dielectric environment. Furthermore, the red and blue shifts of indoline's excitation wavelength in DMSO and water, respectively, can be understood by the participation of the nitrogen lone pair in the solute's electronic structure. The hydrogen-bond accepting ability of DMSO leaves the indoline nitrogen's lone pair isolated

(49) Steel, W. H.; Beildeck, C. L.; Walker, R. A. *J. Phys. Chem. B* **2004**, *108*, 16107.
(50) Zybill, C. E.; Ang, H. G.; Lan, L.; Choy, W. Y.; Meng, E. F. K. *J. Organomet. Chem.* **1997**, *547*, 167.
(51) Moad, A. J.; Simpson, G. J. *J. Phys. Chem. B* **2004**, *108*, 3548.
(52) , Frisch, M. J.; et al. *Gaussian 03*, revision D.01; Gaussian, Inc.: Wallingford, CT, 2004.
(53) Gilli, G.; Gilli, P. *J. Mol. Struct.* **2000**, *552*, 1.
(54) Zheng, Y. J.; Merz, K. M. *J. Comput. Chem.* **1992**, *13*, 1151.
(55) Markovitch, O.; Agmon, N. *Mol. Phys.* **2008**, *106*, 485.

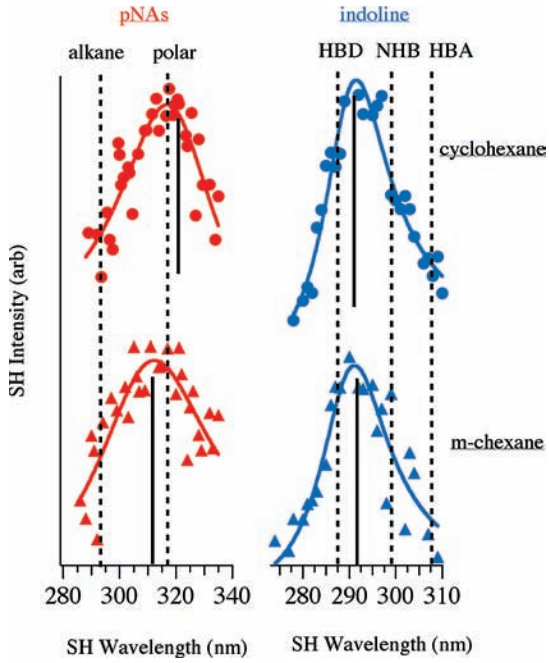

Figure 3. SHG data from pNAs (left) and indoline (right) adsorbed to silica/cyclohexane interfaces (top) and silica/methylcyclohexane (bottom) interfaces. The "polar" and "alkane" dashed lines in the pNAs spectra denote excitation wavelengths in bulk water and alkane solvents, respectively. "HBD", "NHB", and "HBA" labels on the dashed lines in the indoline spectra denote excitation wavelength limits in hydrogen bond donating, non-hydrogen bonding, and hydrogen bond accepting solvents. The black solid lines represent excitation wavelengths of the different solutes at solid/liquid interfaces. Note that differences between intensity maxima in the spectra and the calculated excitation wavelengths can result from a nonresonant contribution to the $\chi^{(2)}$ tensor as shown in eq 3.

and inductively promotes lone pair delocalization into the aromatic ring following excitation. The resulting larger change in permanent dipole leads to a shift in excitation to lower energies (and longer wavelength). In contrast, the hydrogen bond donating property of water stabilizes indoline in its ground state thereby increasing the energetic gap between ground and excited electronic states leading to the experimentally observed blue shift in excitation wavelength.[21,56,57]

3.2. Polarity and Hydrogen Bonding at Alkane/Silica Interface. The data in Figure 1 show pNAs to be very sensitive to its local dielectric environment while indoline samples hydrogen bonding opportunities. Figure 3 shows SHG spectra of pNAs and indoline adsorbed to the silica/cyclohexane and silica/methylcyclohexane interfaces. For pNAs the dashed vertical lines represent excitation wavelengths of the solute in both polar (water) and nonpolar (alkane) limits. The solid vertical lines indicate the excitation wavelength maximum resulting from fitting the data to eqs 2−5. Nonzero contributions from the nonresonant piece of $\chi^{(2)}$ can lead to asymmetry in the band profiles, meaning that the interfacial excitation wavelength does not always match the wavelength having maximum signal intensity in the SHG spectra. Excitation wavelengths from all bulk solution and surface measurements are summarized in Table 2.

Spectra in Figure 3 show that pNAs samples distinctly different nonspecific solvation environments at the interface between silica and these two solvents. Based on their static dielectric constants, cyclohexane (2.02) and methylcyclohexane (2.01) have virtually identical polarities as reflected by equivalent maximum absorption wavelengths of pNAs in both solvents (293 nm). At the silica/cyclohexane interface, however, pNAs experiences a more polar environment ($\lambda_{SHG} = 321 \pm 3$nm) compared to the less polar interface formed between silica and methylcyclohexane ($\lambda_{SHG} = 312 \pm 3$nm). Using data in Figure 1 to approximate an effective interfacial polarity for both of these systems, we find that the cyclohexane/silica interface is even more polar than an aqueous environment ($f(\varepsilon) \approx 1.0$) whereas the methylcyclohexane/silica interface has a dipolar environment corresponding to a local Onsager function of 0.9. With its high density of silanol groups one might expect the interfacial polarity to be close to that of a polar, protic solvent such as water. However, the spectra of pNAs adsorbed to these different silica alkane interfaces show that nonspecific solvation at these boundaries depends on solvent structure as well as solute/substrate interactions.

Surface silanol groups can contribute to the local dipolar environment in several ways. First, surface silanol groups represent a dense collection of immobile dipoles that can polarize the interfacial solute (and solvent) creating a local dielectric environment more polar than bulk solution. Surface silanol groups can also donate and/or accept hydrogen bonds. The collective effect of these contributions to interfacial polarity is reported by adsorbed pNAs, a solute chosen to probe nonspecific or spatially averaged interactions. Indoline's electronic structure, however, is capable of differentiating the general dielectric effects from hydrogen-bond donating and accepting interactions. The right side of Figure 3 shows the SHG spectra of indoline adsorbed to the silica/cyclohexane and silica/methylcyclohexane interfaces. In these spectra vertical dashed lines indicate the absorption maxima in bulk water (288 nm), non-hydrogen bonding solvents such as alkanes and acetonitrile, 299 nm), and DMSO (307 nm). These solvents are chosen to reflect limiting cases for indoline in hydrogen bond donating (HBD), non-hydrogen bonding (NHB), and hydrogen bond accepting (HBA) environments, respectively. The spectra are fit as described above with excitation maxima marked by solid vertical lines. Both spectral fits have maxima at 291 ± 2 nm, a result characteristic of a strong hydrogen bond donating environment.

We attribute these specific solvation effects to the hydrogen-bond donating properties of the surface silanol groups of the silica substrate, although we cannot rule out contributions from water strongly bound to the silica substrate. Supporting our assignment are several studies that report on highly acidic

Table 2. Second Harmonic Data for pNAs and Indoline Adsorbed to Alkane/Silica and *n*-Alcohol Silica Interfaces[a]

			λ (bulk, nm)		λ (surface, nm)	
solvent	ϵ	$f(\epsilon)$	pNAs	indoline	pNAs	indoline
cyclohexane	2.04	0.41	293	299	321 ± 2	291 ± 2
methyl-cyclohexane	2.03	0.41	294	299	312 ± 3	291 ± 2
1-octanol	10.3	0.82	305	295	297 ± 2 320 ± 3	287 ± 2
1-propanol	20.5	0.91	310	293	307 ± 2 320 ± 4	290 ± 3
cyclohexane/ hydrophobic						302 ± 3

[a] Bulk and surface excitation wavelengths of pNAs and indoline adsorbed to different solid/liquid interfaces. SHG data result from fitting data shown in Figures 3, 4, and 6 with eqs 2−5 in text.

(56) Allen, M. W.; Bothwell, T. G.; Slaughter, B. D.; Johnson, C. K. *Biophys. J.* **2002**, *82*, 428.
(57) Slaughter, B. D.; Allen, M. W.; Lushington, G. H.; Johnson, C. K. *J. Phys. Chem. A* **2003**, *107*, 5670.

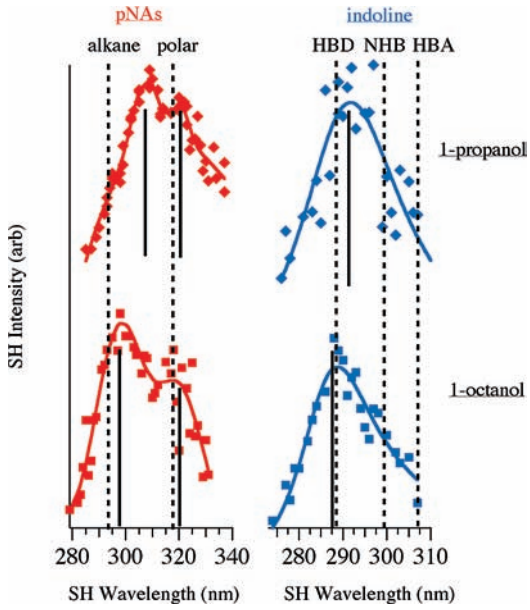

Figure 4. SHG data from pNAs (left) and indoline (right) adsorbed to silica/1-propanol interfaces (top) and silica/1-octanol (bottom) interfaces. Other markings as in Figure 3. Data for pNAs were fit to two distinct electronic resonances. Similar efforts to fit the indoline data to two features resulted in the second feature always having amplitudes >10× smaller than the primary feature.

properties of surface silanol groups on chromatographic silica.[58] As well as the fact that the polarity-dependent results show clear differences in the interfacial dielectric environments, even for different alkanes having equivalent bulk solvating properties. If interfacial water was responsible for the observed hydrogen bond donating properties of the surface, we might expect the polarities of both interfaces (silica/cyclohexane and silica/methylcyclohexane) to be similar.[59,60] Regardless of the source of the strong hydrogen bond donating properties, the data in Figure 3 show clearly that interfacial solvation differs considerably from bulk solution limits *and* interfacial effects on solvation *are not* the same for different solutes.

To further explore the dependence of nonspecific and specific solvation on solvent structure, we examined the solvatochromic responses of pNAs and indoline at interfaces formed between hydrophilic silica and solvents capable of interacting strongly with the solid substrate. Figure 4 compares the SHG spectra of pNAs and indoline at interfaces formed between silica and 1-octanol and between silica and 1-propanol. Unlike the spectrum from the silica/cyclohexane interface that shows only a single electronic resonance, the SHG spectra of pNAs at silica/1-octanol and silica/1-propanol interfaces can only be fit with two contributing features having the same phase. The higher intensity features show maxima centered at 297 ± 3 nm and 307 ± 3 nm for octanol and propanol, respectively, and the lower intensity peaks appear at ~320 nm for both solid/liquid systems. That there are two features in the silica/alcohol spectra is not surprising. Previous studies have reported similar heterogeneous environments at hydrophilic solid/protic solvent, solid/liquid interfaces.[11,12,31] Creation of these microscopic domains having dramatically varying properties has been ascribed to surface induced polar ordering of the interfacial solvent species.[61,62]

Based on the data in Figure 4 as well as related findings from previous reports, we conclude that pNAs adsorbed to silica/1-octanol and silica/1-propanol interfaces samples two distinct polarities: one having a high effective dielectric constant ($f(\epsilon_{eff}) \approx 1.0$ and $\epsilon_{eff} > 80$) and the other being distinctly nonpolar ($f(\epsilon_{eff}) \approx 0.5$ and $\epsilon_{eff} \approx 4$ for 1-octanol; $f(\epsilon_{eff}) \approx 0.8$ and $\epsilon_{eff} \approx 9$ for 1-propanol). The lack of interference between the two features implies that pNAs monomers in the two different dipolar environments share similar orientations, and orientation measurements of pNAs at the silica/1-octanol interface presented below further support this claim.

This result supports a picture of interfacial solvent structure where the −OH groups of the alcohol solvent hydrogen bond to the silica substrate and the chains organize to form a Langmuir-like film that is responsible for the nonpolar environment sampled by the solute. The solutes then partition into the nonpolar region with some monomers continuing to interact strongly with the silica substrate. If relative band intensities reflect approximate populations, one would conclude that, for both silica/1-octanol and silica/1-propanol, more pNAs samples the nonpolar environment. Such a conclusion would be consistent with partitioning studies that show pNAs to be ~20× more soluble in alkanes than in water.[49] However, this interpretation neglects the effects of average solute orientation on SH intensity, and the higher intensity may simply reflect a more upright orientation of the pNAs in the nonpolar region leading to a larger projection of its hyperpolarizability on the surface normal. Average solute orientation results determined from polarization dependent changes in SHG intensity described below support the claim that differences in peak intensities are due to population differences and not changes in solute orientation.

The heterogeneities in polarity observed across silica/alcohol interfaces are not reflected in hydrogen bonding opportunities across these same boundaries. Figure 4 also shows the SH spectra of indoline adsorbed to the same silica/1-octanol and silica/1-propanol interfaces. Dashed lines indicate bulk excitation limits in hydrogen bond donating, non-hydrogen bonding, and hydrogen bond accepting environments, and solid vertical lines represent excitation wavelength maxima. The distinctive environments indicating clear differences in *nonspecific* solvation at the silica/1-octanol and silica/1-propanol interfaces are absent in the data from indoline adsorbed to these same boundaries. Indoline at the silica/1-octanol interface has a single maximum at 287 ± 2 nm in its SH spectrum. This λ_{max} is shifted slightly beyond the strong hydrogen bond donating limit represented by a bulk aqueous solvent. For the case of silica/1-propanol, the SH maximum falls at 290 ± 2 nm. This observation provides additional evidence that specific solvation forces at these polar solid/liquid interfaces depend largely on solute−substrate interactions with little contribution from the solvent itself. We propose that the small but reproducible shift of the indoline solvatochromic data beyond the strong hydrogen bonding limit at the silica/1-octanol interface arises from reduced solute mobility. Strong hydrogen bonding between the silica substrate and the interfacial octanol solvent creates a well ordered monolayer that should be subject to fewer solvent fluctuations and allow for stronger hydrogen bond formation. Based on the

(58) Wirth, M. J.; Piasecki-Coleman, D. A.; Montgomery, M. E. *Langmuir* **1995**, *11*, 990.
(59) Allara, D. L.; Parikh, A. N.; Rondelez, F. *Langmuir* **1995**, *11*, 2357.
(60) Ye, S.; Nihonyanagi, S.; Uosaki, K. *Phys. Chem. Chem. Phys.* **2001**, *3*, 3463.
(61) Benjamin, I. *Chem. Rev.* **2006**, *106*, 1212.
(62) Michael, D.; Benjamin, I. *J. Phys. Chem.* **1995**, *99*, 16810.

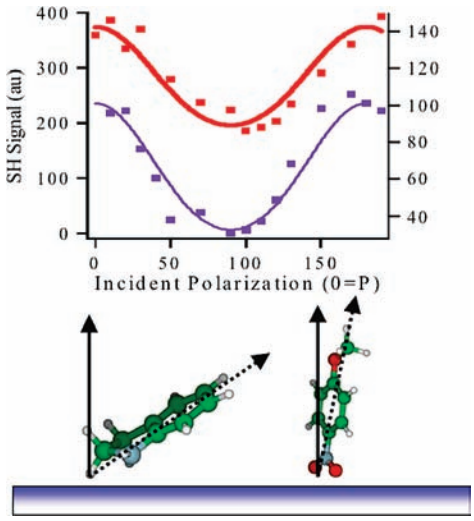

Figure 5. Orientation data for pNAs (top) and indoline (bottom) at the silica/cyclohexane interface. The data were collected by varying the incident light polarization angle from P (0°) to S (90°) then back to P (180°), while observing the P-polarized SH signal. (P-polarized light corresponds to light with its electric field vector in the plane defined by the surface normal and the light propagation direction.) Data are fit to eq 8 to determine the individual contributions to the surface nonlinear susceptibility. The primary difference between the two data are differences in amplitude, with the overall intensity from pNAs being larger (left axis) than indoline (right axis). Also shown are representative figures illustrating pNAs in a mostly upright orientation and indoline lying relatively flat to optimize hydrogen bonding opportunities.

1-octanol vs 1-propanol differences, we surmise that the hydrogen bonds formed between the indoline's nitrogen lone pair and the interfacial H-bond donors are weaker at the silica/1-propanol interface, a result that stands in contrast to the specific solvation interactions observed in bulk solution (see Figure 1).

Experiments to clarify further the different types of solvation present at silica/organic solvent interfaces measured the polarization dependent SH response as a function of incident fundamental polarization. Representative data from experiments measuring the P-polarized SHG signal as a function of incident fundamental polarization for pNAs and indoline at the silica/cyclohexane interface are shown in Figure 5. Together with the measurement of the S-polarized SHG signal arising from a visible field polarized 45° relative to the surface normal (containing both S and P components), the individual components of the surface nonlinear susceptibility tensor can be calculated according to eqs 6−8:

$$\chi^{(2)}_{pss} = L_{zz}L_{xx}L_{xx}\sin\theta_{SH}\chi_{zxx} \tag{6}$$

$$\chi^{(2)}_{sps} = L_{xx}L_{zz}L_{xx}\sin\theta_{SH}\chi_{xzx}$$

$$\chi^{(2)}_{ssp} = L_{xx}L_{xx}L_{zz}\sin\theta_{SH}\chi_{xxz} \tag{7}$$

$$\begin{aligned}\chi^{(2)}_{ppp} = &-L_{xx}L_{xx}L_{zz}\cos\theta_{SH}\cos\theta_{vis}\sin\theta_{vis}\chi_{xxz} - \\ &L_{xx}L_{zz}L_{xx}\cos\theta_{SH}\cos\theta_{vis}\sin\theta_{vis}\chi_{xzx}\ldots + \\ &L_{zz}L_{xx}L_{xx}\sin\theta_{SH}\cos\theta_{vis}\cos\theta_{vis}\chi_{zxx} + \\ &L_{zz}L_{zz}L_{zz}\sin\theta_{SH}\sin\theta_{vis}\sin\theta_{vis}\chi_{zzz}\end{aligned} \tag{8}$$

where L_{ii} are the nonlinear Fresnel factors for the second harmonic and incident light.[44,51,63]

Relating the elements of the macroscopic $\chi^{(2)}$ tensor to the elements of molecular hyperpolarizability, β, requires knowledge about the electronic structure of the molecule itself. With this information, the measured surface nonlinear susceptibility can be related to the molecular hyperpolarizability using a coordinate transformation involving the Euler rotation matrix:

$$\chi^{(2)}_{ijk} = N_s\sum_{i'j'k'}\langle R_{ii'}R_{jj'}R_{kk'}\rangle\beta^{(2)}_{i'j'k'} \tag{9}$$

Table 3. Orientation of pNAs and Indoline at Selected Solid/Liquid Interfaces[a]

solute	solvent	λ (nm)	orientation
pNAs	cyclohexane	321	19° ± 5°
pNAs	1-octanol	297	≤9°
	1-octanol	321	≤9°
indoline	cyclohexane	291	150° ± 5°

[a] Orientation results for pNAs and indoline at silica/cyclohexane and silica/1-octanol interfaces using data shown in Figure 5 and eqs 6−9 in text.

We employed *ab initio* methods described above to calculate the nonzero (gas phase) β_{ijk} elements for both pNAs and indoline. Consistent with its pseudo-C_{2v} structure, the hyperpolarizability of pNAs is dominated by two terms β_{zzz} and β_{zxx} ($=\beta_{zyy}$) where $\beta_{zzz} \gg \beta_{zxx}$. In contrast, indoline has 10 nonzero β elements of significant magnitudes. Consequently, determination of indoline's orientation required a more detailed analysis as described by Simpson and co-workers. [51] (A listing of the nonzero β elements for both pNAs and indoline appear in the Supporting Information.) In all of our calculations, we assumed a delta function distribution, despite the fact that the silica surfaces are not atomically flat and the actual orientations will vary with the specific nature and strength of solute/substrate and solvent/substrate interactions.

The polarization dependent intensities and resulting orientation calculations lead to an average orientation of the molecular electronic transition dipole. Results are reported in Table 3 and illustrated schematically in Figure 5. For all of the solid/liquid systems studied, pNAs adopts a mostly upright geometry with an average orientation of the molecular long axis (= the molecular *a* axis) relative to surface normal of 19 ± 5° at the silica/cyclohexane interface and less than 10° at the silica/1-octanol interface *at both wavelength maxima*. Here the "molecular long axis" corresponds to pNAs' principal *a* axis that runs almost parallel to a line bisecting the nitrogen of the nitro group and the oxygen of the methoxy group. This result suggests that despite the distinctly different dielectric environments present at the silica/1-octanol interface, the average orientations for both adsorbed pNAs populations are quite similar, thus supporting the argument that observed differences in intensities arise from differences in population.

Analysis of the indoline data shows this solute to adopt a more horizontal orientation at the silica/cyclohexane interface. Orientation measurements lead to an average molecular orientation of indoline's principal *a* axis of 150 ± 5° away from the surface normal. This result directs indoline's 2° amine toward the silica surface where it can accept hydrogen bonds from surface silanol groups, consistent with the observed SHG data presented in Figures 4 and 5. We note that both of these results (10°−20° for pNAs and 150° for indoline) lie far from the 39° "magic angle" predicted by Simpson and Rowlen for rough surfaces that lead to a macroscopically random distribution of solute orientation angles.[64] Consequently, we infer that both pNAs and indoline experience a high degree of polar ordering at these strongly associating, polar silica surfaces.

The last experiment conducted in this study was designed to test the contributions of the silica substrate to specific solvation

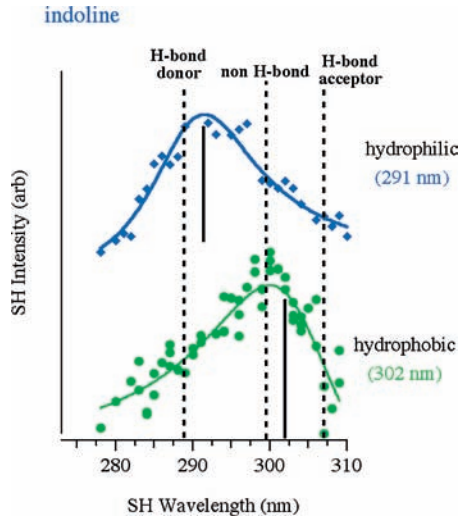

Figure 6. SHG data for indoline adsorbed to the hydrophilic silica/cyclohexane interface (top) and to the hydrophobic silica/cyclohexane interface. The hydrophobic surface was created by exposing overnight a hydrophilic silica prism surface to a vapor saturated with $Si(CH_3)_2Cl_2$. A picture of the contact angle formed with this surface by water is shown in the Supporting Information. The hydrophilic silica/cyclohexane data are the same as those shown in the top, right panel of Figure 3.

forces at the solid/liquid interface. Previous reports in the literature have indicated that polarity at hydrophobic solid surfaces is much lower than bulk solution limits.[65] We eliminated the substrate's ability to donate hydrogen bonds by allowing a film of dimethyldichlorosilane to chemisorb to the silica substrate. Static contact angles formed between water and this surface measured 105°.[50] (A picture used to measure contact angles appears in the Supporting Information.) Figure 6 shows the results of SHG spectra of indoline at both the hydrophilic silica/cyclohexane and hydrophobic silica/cyclohexane interfaces. The bulk limits are shown, along with the SHG maxima. For indoline at hydrophobic silica, λ_{max} shifts to 302 ± 3 nm. This result falls between the non-hydrogen bonding and hydrogen bond accepting bulk limits of 300 and 307 nm, respectively. In principle, methyl terminated silica can still accept hydrogen bonds, but the surface's ability to donate hydrogen bonds, however, is largely eliminated.

These results provide deeper insight into studies of surface diffusion studies of single molecules reported by Wirth and co-workers who characterized solute mobility at hydrocarbon terminated, silica surfaces.[35,39,40] Using a variety of methods including single molecule fluorescence spectroscopy and fluorescence correlation spectroscopy, these investigators found that silica surfaces terminated with long-chain dimethylsilanes still possessed sites capable of strongly binding charged dye molecules from solutions. The strongest of these binding sites were assigned to topographical inhomogeneities resulting from mechanical polishing. The authors proposed that these binding sites were correlated with the isolated or weakly hydrogen-bonded silanol groups reported by Harris and co-workers in the latter's study of pyridine adsorption to silica surfaces.[36,38] Our solvatochromic results contain no direct information about interfacial topography, but the data point clearly to the importance of hydrogen-bond donating properties of silica surfaces in controlling specific solvation interactions compared to the surface's overall polarity and ability to accept hydrogen bonds.

4. Conclusions

Data presented above provide direct, quantitative evidence differentiating various solvation mechanisms that occur at polar solid surfaces. The electronic structure of pNAs at weakly and strongly associating interfaces shows that solvent structure and identity play important roles in controlling the local dipolar environment. When a solution of pNAs in a nonpolar (alkane) solvent is brought into contact with hydrophilic silica, the interfacial region assumes a distinctly polar character although the magnitude of the effect depends on solvent structure. This result supports a model where the polar silica surface creates a high-dielectric environment. However, this model begins to break down when a solution having a more polar, protic solvent is brought into contact with the silica substrate. Alcohol solvents create heterogeneous dipolar environments where one region can be distinctly "alkane-like". The second region remains extremely polar. The nature of this nonpolar region depends on solvent structure and is enhanced with longer-chain alcohol solvents. Solutes sensitive to specific solvation forces do not experience the same solvent-dependent variation in interfacial solvation. Indoline's solvation at the polar silica/liquid interface is homogeneous and appears to be dominated by the hydrogen bond donating properties of the substrate itself and is largely unaffected by the solvent. Only by rendering the silica surface hydrophobic does the nature of the specific solvation at the solid/liquid interface change.

Acknowledgment. The authors gratefully acknowledge support for this work from the National Science Foundation (CHE0608122). R.A.W. thanks the Institute of Advanced Study at Durham University (UK) for Fellowship support during the initial stages of manuscript preparation. The authors also thank Professor D. Kosov (University of Maryland), Professor C. Johnson (University of Kansas), and Professor J. Foresman (York College, PA) for their invaluable assistance with various aspects of the *ab initio* calculations reported in this work.

Supporting Information Available: Complete biliographic information for ref 52 (Gaussian03) can be found in the Supporting Information. Also in the Supporting Information is the procedure for creating the hydrophobic surfaces used in the experiments reported in Figure 6, and a picture used to determine contact angles with an aqueous solvent. Also listed are the nonzero elements of the molecular hyperpolarizabilities of pNAs and indoline. Orientation data acquired at two different wavelengths from pNAs adsorbed the silica/1-octanol interface are also presented. This material is available free of charge via the Internet at http://pubs.acs.org.

JA810117F

(63) Simpson, G. J.; Perry, J. M.; Ashmore-Good, C. L. *Phys. Rev. B* **2002**, 66.
(64) Simpson, G. J.; Rowlen, K. L. *Acc. Chem. Res.* **2000**, *33*, 781.
(65) Zhang, X. Y.; Esenturk, O.; Walker, R. A. *J. Am. Chem. Soc.* **2001**, *123*, 10768.